Systems & Control Letters 62 (2013) 482–495

Contents lists available at SciVerse ScienceDirect

Systems & Control Letters

journal homepage: www.elsevier.com/locate/sysconle

Exact stability analysis of second-order leaderless and leader–follower consensus protocols with rationally-independent multiple time delays☆

Rudy Cepeda-Gomez [a], Nejat Olgac [b,*]

[a] Department of Mechatronic Engineering, Universidad Santo Tomas, Bucaramanga, Colombia

[b] Mechanical Engineering Department, University of Connecticut, Storrs, CT 06268, USA

ARTICLE INFO

Article history:
Received 1 May 2012
Received in revised form
20 November 2012
Accepted 15 February 2013

Keywords:
Delay
Rationally-independent delays
CTCR
Consensus
Directed topology

ABSTRACT

An investigation of double-integrator agents with directed asymmetric consensus protocols and multiple rationally independent time delays is presented in this paper from two novel perspectives. First, we complement the group consensus literature on crucial stability analysis, using a recent technique called the Cluster Treatment of Characteristic Roots (CTCR) for the first time on this class of time-delayed systems. The CTCR paradigm is pursued after a block-diagonalization (mode-decoupling) transformation on the system. This treatment produces some unique stability tables for the dynamics in the space of the delays which are non-conservative and exhaustive. Second, a novel concept of spectral delay space is presented, as an overture to the CTCR for the determination of the complete set of stability-crossing (switching) hypersurfaces in the delay space. Examples are provided to display the strengths and efficiency of this new stability analysis mechanism.

1. Introduction

The consensus problem for multi-agent systems, a subtopic of the field of cooperative control, has received a great deal of attention in recent years. Following the work of Olfati-Saber and Murray [1], many researchers have contributed to the knowledge in this area. Some of these studies are limited to the systems with first-order agents [1,2], while others focus on second-order agent behavior [3]; some also include time delays in the communication channels [3,4]. In particular, there is a large volume of literature on the stability of time-delayed dynamics. However, very few works, such as [5–7], offer a practicable procedure for the exact (non-conservative) assessment of the stability properties of such consensus systems with respect to the delays, when the delays are rationally independent.

Although the treatment is applicable to a much broader range of systems, we focus on a set of generally accepted consensus protocols within this paper. This study presents the first such deployment on group dynamics with directed topologies considering leaderless and leader–follower strategies. Similar to the settings presented in [8], the agents operating under these protocols are assumed to be affected by two rationally independent time delays: a communication delay and an input delay. The communication delay is imposed on the information coming from other agents (both on position and velocity information). The input delay affects all the state feedback, including that of the states of its own agents. Other investigations [9,10] report similar consensus studies, including "diverse" time delays in the topology. Ref. [9] considers only discrete dynamics, and rationally dependent delays, as they are integer multiples of the base delay (sampling period). As such, the ensuing characteristic equations (e.g., Eq. (7) in [9]) are simplified immensely to finite-dimensional polynomials, instead of the infinite-dimensional quasi-polynomials we will present here. From this standpoint the attribute "diverse" is an important misnomer. The more convincing terminology should have been "multiple rationally dependent delays with commensurate conditions [11]". Ref. [10], on the other hand, is a treatment of the leader–follower consensus in a continuous domain. But several aspects of the treatment pose severe restrictions vis-à-vis the present paper: (a) symmetric systems are considered with asymmetric perturbations, which imply that the nominal behavior has to be symmetric, and (b) it uses a generalized Nyquist treatment, which confines the work to a fixed point analysis in the delay space. By contrast, the study presented here is in the free delay space, and stability charts are provided for a wide range of delays. Another study [12] also presents a solution to the consensus stability problem under multiple delays in the topology. That treatment, however, is confined to undirected topologies only, as the authors of [12] state

☆ This work was supported in part by ARO grant W911NF-07-1-0557.

* Corresponding author. Tel.: +1 8604862382; fax: +1 8604865088.
E-mail addresses: rudycepeda@engr.uconn.edu (R. Cepeda-Gomez), olgac@engr.uconn.edu (N. Olgac).

0167-6911/$ – see front matter © 2013 Elsevier B.V. All rights reserved.
http://dx.doi.org/10.1016/j.sysconle.2013.02.011

that "it is very difficult, if at all possible, to extend the presented method for directed graphs" due to the complex eigenvalues involved. The present paper, on the other hand, tackles directed (as well as undirected) topologies using a completely different approach, which overcomes the "complex eigenvalue" restriction of [12].

The stability analysis utilized in [8] is based on the Lyapunov–Razumikhin theorem; therefore it is conservative. The methodology provides the sufficient conditions for stability, but they are not necessary. The new technique which is performed here, the Cluster Treatment of Characteristic Roots, CTCR, in contrast, creates exact and exhaustive stability regions in the parametric space [13–15]. It is interesting to note that such a methodology, which can reveal the stability region(s) exhaustively, opens a unique path to another interesting control design tool: *delay scheduling* [16,17]. In essence, this tool offers a strategy of artificially prolonging the existing delays in order to achieve improved stability features. Although such capability is novel, paradoxical and counter-intuitive, we will only present a couple of example cases without getting into details in this text, due to space limitations.

In the rest of the paper, bold face notation is used for vector quantities, bold capital letters for matrices, and italic symbols for scalars.

2. Problem statement and control laws

We consider a group of n agents driven by simple double-integrator dynamics $\ddot{x}_j(t) = u_j(t), j = 1, 2, \ldots, n$, where $x_j(t)$ is the scalar position of the agent and $u_j(t)$ the control input. This paper is presented considering only one-dimensional cases for notational simplicity, but the treatment can be easily scaled up to a higher-dimensional case by using Kronecker product operator as in [18]. It is common in group dynamics studies that the consensus is declared when the agents reach a common position and a common velocity, i.e., when $\lim_{t\to\infty}\left(x_j(t) - x_k(t)\right) = 0$ and $\lim_{t\to\infty}\left(\dot{x}_j(t) - \dot{x}_k(t)\right) = 0$ for any j and k. In order to achieve this objective, the members of the group share their position and velocity information with a limited number of neighbors, through some one-directional communication channels. The group of peer agents from which agent j receives information is called the informers of agent j, denoted by N_j, and this set consists of $\delta_j(< n)$ agents.

The type of communication topology used here can be described by a directed graph with n vertices. The adjacency matrix of this graph is denoted by $\mathbf{A}_\Gamma = \left[a_{jk}\right] \in \Re^{n\times n}$, with $a_{jk} > 0$ whenever agent k is an informer of agent j and $a_{jk} = 0$ otherwise. The diagonal elements are also taken as zero: $a_{jj} = 0$. Notice that this matrix is not necessarily symmetric. The *in-degree matrix* of the graph is a diagonal matrix Δ, with $\Delta_{jj} = \sum_{k=1}^{n} a_{jk}$.

For this multi-agent system, four different control logics are suggested considering leaderless and leader–follower cases. These control laws are presented next, in order to establish the foundations of this investigation.

2.1. *Case A*, Leaderless consensus

All agents are equal, and they drive themselves using a weighted feedback on relative errors. The control logic utilized by the agents is taken from [8]:

$$u_j(t) = -\frac{1}{\Delta_{jj}}\sum_{k=1}^{n} a_{jk}\left(x_j(t-\tau_{in}) - x_k(t-\tau_{in}-\tau_{com})\right) - \frac{\gamma}{\Delta_{jj}}\sum_{k=1}^{n} a_{jk}\left(\dot{x}_j(t-\tau_{in}) - \dot{x}_k(t-\tau_{in}-\tau_{com})\right), \quad (1)$$

where τ_{in} and τ_{com} are the input and communication delays, respectively, and γ is a positive ratio between the derivative and position error gains. It is also assumed that each agent has at least one informer, i.e., $\Delta_{jj} \neq 0$ for $j = 1, 2, \ldots, n$. The control logic (1) can be expressed in state space as

$$\dot{\mathbf{x}}(t) = \left(\mathbf{I}_n \otimes \begin{bmatrix} 0 & 1 \\ 0 & 0 \end{bmatrix}\right)\mathbf{x}(t) + \left(\mathbf{I}_n \otimes \begin{bmatrix} 0 & 0 \\ -1 & -\gamma \end{bmatrix}\right)\mathbf{x}(t-\tau_1) + \left(\mathbf{C} \otimes \begin{bmatrix} 0 & 0 \\ 1 & \gamma \end{bmatrix}\right)\mathbf{x}(t-\tau_2), \quad (2)$$

where $\mathbf{x} = [x_1\dot{x}_1x_2\dot{x}_2\cdots x_n\dot{x}_n] \in \Re^{2n}$ is the state vector. In (2), $\mathbf{I}_n$ represents the identity matrix of order n, $\otimes$ is the Kronecker product operation [18], and $\mathbf{C} = \boldsymbol{\Delta}^{-1}\mathbf{A}_\Gamma$. Notice the renaming of the rationally independent delays for convenience, as $\tau_1 = \tau_{in}$ and $\tau_2 = \tau_{in} + \tau_{com}$. An important feature of this control logic is that the final position of the agents is dictated by their initial conditions and the communication structure, as in a typical consensus protocol [8].

2.2. *Case B*, Consensus regulation with constant final velocity

The remaining cases in Sections 2.2–2.4 are consensus problems in the "leader–follower" class in which it is assumed that there is a virtual leader, labeled as agent $n + 1$, and the other agents behave in accordance with it. The particularities of the consensus may vary (e.g., position tracking or velocity agreement), and they are described for each case next.

In **case B**, the motion of the leader is described by a position $x_{n+1}(t) = r_d(t)$ and constant velocity $\dot{x}_{n+1}(t) = v_d$. The objective of the control is to guarantee that all the agents in the group track the virtual leader. For this case, and all the other leader–follower cases, the adjacency matrix is augmented with an extra column to indicate which agents are receiving position and velocity information from the virtual leader. This new adjacency matrix is denoted $\mathbf{A}_{\Gamma+1} = \left[a_{jk}\right] \in \Re^{n\times(n+1)}$. The elements in the first n columns declare the interactions between the agents, and the elements in the last column are defined as $a_{j,n+1} > 0$ if agent j has access to the virtual leader and $a_{j,n+1} = 0$ otherwise. The n-dimensional diagonal in-degree matrix for this case is defined similarly as in the leaderless case, with $\Delta_{jj} = \sum_{k=1}^{n+1} a_{jk}$.

The proposed control law is

$$u_j(t) = -\frac{1}{\Delta_{jj}}\sum_{k=1}^{n+1} a_{jk}\left(x_j(t-\tau_{in}) - x_k(t-\tau_{in}-\tau_{com})\right) - \frac{\gamma}{\Delta_{jj}}\sum_{k=1}^{n+1} a_{jk}\left(\dot{x}_j(t-\tau_{in}) - \dot{x}_k(t-\tau_{in}-\tau_{com})\right) \quad (3)$$

for $j = 1, 2, \ldots, n$. It is also taken from [8]. Again, τ_{in} and τ_{com} are the input and communication delays, respectively, and $\gamma > 0$. It is again assumed that $\Delta_{jj} \neq 0$ for every agent.

By using the state vector $\mathbf{x} = [x_1\dot{x}_1x_2\dot{x}_2\cdots x_n\dot{x}_n] \in \Re^{2n}$, the control law (3) can be expressed in state space as

$$\dot{\mathbf{x}}(t) = \left(\mathbf{I}_n \otimes \begin{bmatrix} 0 & 1 \\ 0 & 0 \end{bmatrix}\right)\mathbf{x}(t) + \left(\mathbf{I}_n \otimes \begin{bmatrix} 0 & 0 \\ -1 & -\gamma \end{bmatrix}\right)\mathbf{x}(t-\tau_1) + \left(\hat{\mathbf{C}} \otimes \begin{bmatrix} 0 & 0 \\ 1 & \gamma \end{bmatrix}\right)\mathbf{x}(t-\tau_2) + \left(\hat{\mathbf{c}}_{n+1} \otimes \begin{bmatrix} 0 \\ x_d(t-\tau_2) + \gamma v_d \end{bmatrix}\right), \quad (4)$$

where $\hat{\mathbf{C}} = \boldsymbol{\Delta}^{-1}\mathbf{A}_\Gamma \in \Re^{n\times n}$ and $\hat{\mathbf{c}}_{n+1} = \boldsymbol{\Delta}^{-1}\mathbf{a}_{n+1} \in \Re^{n}$. Here, $\mathbf{A}_\Gamma \in \Re^{n\times n}$ includes the first n columns of the adjacency matrix $\mathbf{A}_{\Gamma+1}$, and $\mathbf{a}_{n+1} \in \Re^{n\times 1}$ is its last column.

Notice that (4) can be seen as a special case of (2) in which a forcing term, corresponding to the dynamics of the virtual leader, is added. This term, however, does not affect the stability of the consensus problem, as it is independent of the state $\mathbf{x}(t)$. It is only a driving term in the dynamics. As such, it simply defines the final agreement value.

2.3. **Case C**, Consensus tracking with full access to the virtual leader

In this case, the virtual leader is assumed to be moving with time-variant velocity. Its trajectory is defined such that its velocity $\dot{x}_{n+1}(t) = v_d(t)$, its acceleration $\ddot{x}_{n+1}(t) = \dot{v}_d(t)$, and the derivative of acceleration $\ddot{v}_d(t)$ are bounded. Full access implies that all the agents have information about the acceleration of the virtual leader. However, its position and velocity are available only to a selected group of agents, defined by the $n+1$th column of the adjacency matrix $\mathbf{A}_{\Gamma^*+1}$.

The control logic we consider is

$$\begin{aligned} u_j(t) = & -\frac{1}{\Delta_{jj}}\sum_{k=1}^{n+1} a_{jk}\left(x_j(t-\tau_{in}) - x_k(t-\tau_{in}-\tau_{com})\right) \\ & -\frac{\gamma}{\Delta_{jj}}\sum_{k=1}^{n+1} a_{jk}\left(\dot{x}_j(t-\tau_{in}) - \dot{x}_k(t-\tau_{in}-\tau_{com})\right) \\ & +\ddot{x}_{n+1}(t-\tau_{in}-\tau_{com}), \end{aligned} \tag{5}$$

which can be expressed in state space as

$$\begin{aligned} \dot{\mathbf{x}}(t) = & \left(\mathbf{I}_n \otimes \begin{bmatrix} 0 & 1 \\ 0 & 0 \end{bmatrix}\right)\mathbf{x}(t) + \left(\mathbf{I}_n \otimes \begin{bmatrix} 0 & 0 \\ -1 & -\gamma_t \end{bmatrix}\right) \\ & \mathbf{x}(t-\tau_1) + \left(\hat{\mathbf{C}} \otimes \begin{bmatrix} 0 & 0 \\ 1 & \gamma \end{bmatrix}\right) \\ & \mathbf{x}(t-\tau_2) + \mathbf{1}_{n\times 1} \otimes \begin{bmatrix} 0 \\ \ddot{x}_d(t-\tau_2) \end{bmatrix} \\ & + \left(\hat{\mathbf{c}}_{n+1} \otimes \begin{bmatrix} 0 \\ x_d(t-\tau_2) + \gamma\dot{x}_d(t-\tau_2) \end{bmatrix}\right), \end{aligned} \tag{6}$$

where $\mathbf{1}_{n\times 1}$ is an $n \times 1$ column vector, all the elements of which are equal to 1.

It is evident that (4) and (6) have the same structure; the only difference is in the forcing term which now has an added acceleration term in (6). As in scenario *B*, the driving terms do not influence the stability of the group.

2.4. **Case D**, Consensus tracking with partial access to the virtual leader

We next consider the case where only a subset of the agents has access to the state of the virtual leader. This is achieved by setting $a_{j,n+1} = 1$ for those agents which have access and $a_{j,n+1} = 0$ for the others. However, the latter group uses the acceleration of their informers to obtain an indication of the acceleration of the leader. This particularity brings an interesting twist that only in this scenario does the agent acceleration come into the governing equations with time delay. The resulting time-delayed dynamics becomes *neutral* in nature [11], as we see later. The control law is proposed as

$$\begin{aligned} u_j(t) = & -\frac{1}{\Delta_{jj}}\sum_{k=1}^{n+1} a_{jk}\left(x_j(t-\tau_{in}) - x_k(t-\tau_{in}-\tau_{com})\right) \\ & -\frac{\gamma}{\Delta_{jj}}\sum_{k=1}^{n+1} a_{jk}\left(\dot{x}_j(t-\tau_{in}) - \dot{x}_k(t-\tau_{in}-\tau_{com})\right) \\ & +\frac{1}{\Delta_{jj}}\sum_{k=1}^{n+1} a_{jk}\ddot{x}_k(t-\tau_{in}-\tau_{com}). \end{aligned} \tag{7}$$

This logic is similar to that given in Eq. (27) of [8], however with an important difference. In its original form, the input delay is intentionally ignored in order to reduce the complexity and to simplify the stability analysis. In this paper, we include both the communication and input delays, as this inclusion does not impose a problem for the CTCR paradigm.

The state space version of (7) is

$$\begin{aligned} \dot{\mathbf{x}}(t) = & \left(\mathbf{I}_n \otimes \begin{bmatrix} 0 & 1 \\ 0 & 0 \end{bmatrix}\right)\mathbf{x}(t) + \left(\mathbf{I}_n \otimes \begin{bmatrix} 0 & 0 \\ -1 & -\gamma \end{bmatrix}\right) \\ & \mathbf{x}(t-\tau_1) + \left(\hat{\mathbf{C}} \otimes \begin{bmatrix} 0 & 0 \\ 1 & \gamma \end{bmatrix}\right)\mathbf{x}(t-\tau_2) \\ & + \left(\hat{\mathbf{C}} \otimes \begin{bmatrix} 0 & 0 \\ 0 & 1 \end{bmatrix}\right)\dot{\mathbf{x}}(t-\tau_2) \\ & + \left(\hat{\mathbf{c}}_{n+1} \otimes \begin{bmatrix} 0 \\ x_d(t-\tau_2) + \gamma\dot{x}_d(t-\tau_2) + \ddot{x}_d(t-\tau_2) \end{bmatrix}\right). \end{aligned} \tag{8}$$

The homogeneous part of (8), which dictates the stability posture of the dynamics, includes a delayed component of the highest derivative of the state, making the dynamics a *neutral-type multiple time-delayed system*, NMTDS. This class of systems has some intriguing particularities, which make their stability analysis more cumbersome [19,13,20]. The added complexity does not, however, cause a difficulty for the CTCR process. More details about this will be given in the following sections.

3. Factorization of the characteristic equation

The characteristic equations of the system described, (2), (4), (6) and (8), are $2n$-degree quasi-polynomials in which the delay terms appear with up to $2n$ degrees of commensuracy and with cross-talk terms. Obviously, the complexity of these equations increases rapidly with the number of agents, n. To the best knowledge of the authors, the only paradigm that provides an exact determination of the stability posture of such systems with respect to the time delays is the Cluster Treatment of Characteristic Roots, CTCR [14,15]. The direct deployment of the CTCR to those systems in its original form, however, is still very tedious. Furthermore, the general problem of multiple time delay systems is also known to be NP-hard. Once again, this process becomes numerically intractable as the order of the characteristic equation increases [21]. We circumvent this complication by performing a factorization procedure followed by the application of the CTCR to the simplified system.

The lemma below shows how this factorization methodology is applied to cases *A*, *B*, and *C*. Notice that, in cases *B* and *C*, we are interested only in the homogeneous part of the dynamics, since it determines the stability. Furthermore, this homogeneous part has the same structure as in case *A*. For case *D*, its structure is different (i.e., neutral type), and the application of the respective factorization is presented next.

Lemma 1 (*Factorization Property*)**.** *The characteristic equation of scenarios A, B, and C can always be expressed as the product of a set of second-order and fourth-order factors:*

$$\begin{aligned} Q(s,\gamma,\tau_1,\tau_2) &= \det\left(s\mathbf{I}_{2n} - \mathbf{A} - \mathbf{B}_1 e^{-\tau_1 s} - \mathbf{B}_2 e^{-\tau_2 s}\right) \\ &= \prod_{j=1}^{\ell+m} q_j\left(s,\gamma,\tau_1,\tau_2,\lambda_j\right) \\ &= \prod_{j=1}^{\ell}\left[s^2 + (\gamma s+1)\left(e^{-\tau_1 s} - \lambda_j e^{-\tau_2 s}\right)\right] \\ &\quad \prod_{j=\ell+1}^{m}[s^4 + 2s^2(\gamma s+1)(e^{-\tau_1 s} \\ &\quad - \mathrm{Re}(\lambda_j)e^{-\tau_2 s}) + (\gamma s+1)^2(e^{-2\tau_1 s} \\ &\quad - 2\mathrm{Re}(\lambda_j)e^{-(\tau_1+\tau_2)s} + |\lambda_j|^2 e^{-2\tau_2 s})] = 0, \end{aligned} \tag{9}$$

where matrices $\mathbf{A}$, $\mathbf{B}_1$, *and* $\mathbf{B}_2$ *are self-evident from (2), (4) and (6) in each case (remember, only the homogeneous parts of (4) and (6) are observed) and* λ_j, $j = 1, 2, \ldots, n$, *represent the eigenvalues of the matrix* $\mathbf{C}$ *in case A and the matrix* $\hat{\mathbf{C}}$ *in cases B and C. It is assumed that these matrices have* ℓ *real eigenvalues, denoted by* $j = 1, 2, \ldots, \ell$, *and m complex conjugate eigenvalue pairs,* (λ_j, λ_j^*), $j = \ell+1, \ell+2, \ldots, \ell+m$, $n = \ell + 2m$. *We assume, for simplicity, that each eigenvalue is semi-simple.*

Proof. In this proof, we refer to matrix $\mathbf{C}$, corresponding to case *A*; the results are the same for $\hat{\mathbf{C}}$ in cases *B* and *C*. Let $\mathbf{T}$ be the non-singular similarity transformation matrix that converts $\mathbf{C}$ into its real Jordan canonical form: $\boldsymbol{\Lambda} = \mathbf{T}^{-1}\mathbf{C}\mathbf{T}$. Matrix $\boldsymbol{\Lambda} \in \Re^{n\times n}$ is a block-diagonal matrix, of the form

$$\boldsymbol{\Lambda} = \begin{bmatrix} \lambda_1 & 0 & \cdots & 0 & 0 & \cdots & 0 \\ 0 & \lambda_2 & \cdots & 0 & 0 & \cdots & 0 \\ \vdots & \vdots & \ddots & \vdots & \vdots & \ddots & \vdots \\ 0 & 0 & 0 & \lambda_\ell & 0 & \cdots & 0 \\ \mathbf{0} & \mathbf{0} & \mathbf{0} & \mathbf{0} & \mathbf{J}_{\ell+1} & \cdots & \mathbf{0} \\ \vdots & \vdots & \vdots & \vdots & \vdots & \ddots & \vdots \\ \mathbf{0} & \mathbf{0} & \mathbf{0} & \mathbf{0} & \mathbf{0} & \cdots & \mathbf{J}_{\ell+m} \end{bmatrix}, \tag{10}$$

where $\lambda_j, j = 1, 2, \ldots, \ell$, are the (size-1) Jordan blocks corresponding to the real eigenvalues and

$$\mathbf{J}_j = \begin{bmatrix} \mathrm{Re}(\lambda_j) & -\mathrm{Im}(\lambda_j) \\ \mathrm{Im}(\lambda_j) & \mathrm{Re}(\lambda_j) \end{bmatrix}, \quad j = \ell+1, \ell+2, \ldots, \ell+m \tag{11}$$

are the size-2 Jordan blocks corresponding to the complex conjugate eigenvalue pairs. The first ℓ columns of the matrix $\mathbf{T}$ are composed of the ℓ eigenvectors of matrix *C*. The remaining columns are the generalized real eigenvectors, obtained from the complex conjugate eigenvectors that correspond to the complex eigenvalues [22]. A state transformation $\mathbf{x}(t) = (\mathbf{T}\otimes\mathbf{I}_2)\boldsymbol{\xi}(t)$ in (2) results in

$$\begin{aligned} \dot{\boldsymbol{\xi}}(t) = {} & (\mathbf{T}^{-1}\otimes\mathbf{I}_2)\left(\mathbf{I}_n\otimes\begin{bmatrix}0 & 1\\ 0 & 0\end{bmatrix}\right)(\mathbf{T}\otimes\mathbf{I}_2)\boldsymbol{\xi}(t) \\ & + (\mathbf{T}^{-1}\otimes\mathbf{I}_2)\left(\mathbf{C}\otimes\begin{bmatrix}0 & 0\\ -1 & -\gamma\end{bmatrix}\right)(\mathbf{T}\otimes\mathbf{I}_2)\boldsymbol{\xi}(t-\tau_1) \\ & + (\mathbf{T}^{-1}\otimes\mathbf{I}_2)\left(\mathbf{C}\otimes\begin{bmatrix}0 & 0\\ 1 & \gamma\end{bmatrix}\right)(\mathbf{T}\otimes\mathbf{I}_2)\boldsymbol{\xi}(t-\tau_2). \end{aligned} \tag{12}$$

A convenient property of the Kronecker product [18] is $(\mathbf{U}\otimes\mathbf{V})(\mathbf{W}\otimes\mathbf{Z}) = \mathbf{U}\mathbf{W}\otimes\mathbf{V}\mathbf{Z}$, where $(\mathbf{U}, \mathbf{W})$ and $(\mathbf{V}, \mathbf{Z})$ are square matrices of the same dimensions pairwise. Using this property, (12) becomes

$$\begin{aligned} \dot{\boldsymbol{\xi}}(t) = {} & \left(\mathbf{I}_n\otimes\begin{bmatrix}0 & 1\\ 0 & 0\end{bmatrix}\right)\boldsymbol{\xi}(t) + \left(\mathbf{I}_n\otimes\begin{bmatrix}0 & 0\\ -1 & -\gamma\end{bmatrix}\right) \\ & \boldsymbol{\xi}(t-\tau_1) + \left(\boldsymbol{\Lambda}\otimes\begin{bmatrix}0 & 0\\ 1 & \gamma\end{bmatrix}\right)\boldsymbol{\xi}(t-\tau_2). \end{aligned} \tag{13}$$

Since $\mathbf{I}_n$ and $\boldsymbol{\Lambda}$ are diagonal and block-diagonal matrices, respectively, Eq. (13) is block-diagonalized; thus it can be represented as a set of $\ell + m$ dynamically decoupled subsystems as

$$\begin{aligned} \dot{\boldsymbol{\xi}}_j(t) = {} & \begin{bmatrix}0 & 1\\ 0 & 0\end{bmatrix}\boldsymbol{\xi}_j(t) + \begin{bmatrix}0 & 0\\ -1 & -\gamma\end{bmatrix}\boldsymbol{\xi}_j(t-\tau_1) \\ & + \lambda_j\begin{bmatrix}0 & 0\\ 1 & -\gamma\end{bmatrix}\boldsymbol{\xi}_j(t-\tau_2), \quad \text{for } j = 1, 2, \ldots, \ell \end{aligned} \tag{14a}$$

$$\begin{aligned} \dot{\boldsymbol{\xi}}_j(t) = {} & \left(\mathbf{I}_2\otimes\begin{bmatrix}0 & 1\\ 0 & 0\end{bmatrix}\right)\boldsymbol{\xi}_j(t) + \left(\mathbf{I}_2\otimes\begin{bmatrix}0 & 0\\ -1 & -\gamma\end{bmatrix}\right) \\ & \boldsymbol{\xi}_j(t-\tau_1) + \left(\mathbf{J}_j\otimes\begin{bmatrix}0 & 0\\ 1 & \gamma\end{bmatrix}\right) \\ & \boldsymbol{\xi}_j(t-\tau_2) \quad \text{for } j = \ell+1, \ell+2, \ldots, m. \end{aligned} \tag{14b}$$

The characteristic equation of the complete system therefore becomes a product of $\ell + m$ individual subsystems, which are

$$\begin{aligned} q_j(s, \gamma, \tau_1, \tau_2, \lambda_j) &= s^2 + (\gamma s + 1)\left(\mathrm{e}^{-\tau_1 s} - \lambda_j \mathrm{e}^{-\tau_2 s}\right) \\ &= 0, \end{aligned} \tag{15a}$$

$$\begin{aligned} q_j(s, \gamma, \tau_1, \tau_2, \lambda_j) = {} & s^4 + 2s^2(\gamma s + 1) \\ & \times \left(\mathrm{e}^{-\tau_1 s} - \mathrm{Re}(\lambda_j)\,\mathrm{e}^{-\tau_2 s}\right) \\ & + (\gamma s + 1)^2\left(\mathrm{e}^{-2\tau_1 s} - 2\mathrm{Re}(\lambda_j)\right. \\ & \left. \times\, \mathrm{e}^{-(\tau_1+\tau_2)s} + |\lambda_j|^2 \mathrm{e}^{-2\tau_2 s}\right) = 0, \end{aligned} \tag{15b}$$

corresponding to ℓ of (14a) and m of (14b), respectively. □

Remark. In Lemma 1, we have assumed that the real eigenvalues of matrix $\mathbf{C}$ always create Jordan blocks of size 1. If a multiple real eigenvalue creates a Jordan block of size 2 or larger (which implies that the corresponding eigenvectors are not linearly independent), the relevant characteristic equation factor, similar to (15b), can still be obtained and analyzed. Such instances are, however, extremely rare. Although the procedure remains unchanged, the complexity increases. We ignore further pursuit along this line, within the scope of this work. In the example section, the case of a Jordan block of size 2 arising from complex conjugate eigenvalues is displayed.

A similar procedure to the one described in Lemma 1 can be applied to the homogeneous part of the control logic in case *D*. It leads to factors

$$\begin{aligned} q_j(s, \gamma_{ft}, \tau_1, \tau_2, \lambda_j) = {} & \left(1 - \lambda_j \mathrm{e}^{-\tau_2 s}\right)s^2 + (\gamma s + 1) \\ & \left(\mathrm{e}^{-\tau_1 s} - \lambda_j \mathrm{e}^{-\tau_2 s}\right) = 0 \end{aligned} \tag{16a}$$

for real eigenvalues, and

$$\begin{aligned} q_j(s, \gamma, \tau_1, \tau_2, \lambda_j) = {} & \left(1 - 2\mathrm{Re}(\lambda_j)\,\mathrm{e}^{-\tau_2 s} + |\lambda_j|^2 \mathrm{e}^{-2\tau_2 s}\right)s^4 \\ & + s^2(\gamma s + 1)\left(\mathrm{e}^{-\tau_1 s} - \mathrm{Re}(\lambda_j)\,\mathrm{e}^{-\tau_2 s}\right) + (\gamma s + 1)^2 \\ & \left(\mathrm{e}^{-2\tau_1 s} - 2\mathrm{Re}(\lambda_j)\,\mathrm{e}^{-(\tau_1+\tau_2)s} + |\lambda_j|^2 \mathrm{e}^{-2\tau_2 s}\right) = 0 \end{aligned} \tag{16b}$$

for complex conjugate eigenvalue pairs.

Remark. We want to emphasize here that (16a) and (16b), the factors created in case *D*, have transcendental terms which multiply the highest power of *s*. This implies that the highest-order term in the dynamics is affected by delays. Specifically, (16a) and (16b) become neutral-type quasi-polynomials [11]. The stability analysis of these factors has some extra intricacies when compared to (15a) and (15b). More details will be given in the following sections.

This factorization technique simplifies the problem considerably, by transforming it from a $2n$-order system with time delays of commensuracy degree up to n and delay cross-talk into ℓ second-order and m fourth-order systems with highest commensuracy of 2 (e.g., $\mathrm{e}^{-2\tau_1 s}$) and single-delay cross-talk (e.g., $\mathrm{e}^{-(\tau_1+\tau_2)s}$). Notice that, since the only discriminating element from one factor to the other is the eigenvalue λ_j, the stability analysis in the domain of the delays must be performed only twice, once for a generic real λ and once for a generic complex λ. These tasks are detailed later. The stability problem of the system is now reduced to obtaining the specific eigenvalues of a known matrix $\mathbf{C}$ or $\hat{\mathbf{C}}$, and superposing the

stability outlook of each characteristic equation factor [(15a) and (15b) or (16a) and (16b)] to obtain the ensemble stability tableau for the system.

4. Consensusability and tracking capabilities

In this section, we investigate the conditions which guarantee the consensus when the operation is under protocol *A*, and the agents are able to track the virtual leader when protocols *B*, *C*, or *D* are used.

4.1. Consensusability of protocol A

This discussion is centered on the special features of the eigenvalues of matrix **C**. From the way this matrix is created, any row sum is always 1. This property makes **C** a *row-stochastic matrix* [22]. Using Gershgorin's disk theorem [23], it can be shown that the norm of each eigenvalue is always equal to or less than 1. Furthermore, it has been proven [24] that, if the topology has at least one spanning tree, $\lambda = 1$ is one of the eigenvalues of matrix **C** with multiplicity 1. Then, from (15a), the corresponding

$$q_1(s, \gamma, \tau_1, \tau_2, \lambda = 1) = s^2 + (\gamma s + 1)\left(e^{-\tau_1 s} - e^{-\tau_2 s}\right) = 0 \quad (17)$$

is always a factor in the characteristic quasi-polynomial (9) for protocol *A*. Without loss of generality, we will assign this eigenvalue to the state ξ_1. It can be shown that the normalized eigenvector corresponding to this state is always $\mathbf{t}_1 = 1/\sqrt{n}\begin{bmatrix}1 & 1 & \cdots & 1\end{bmatrix}^T \in \Re^n$, and it is selected as the first column of the earlier defined transformation matrix **T** for this case. Factor (17) governs the dynamics of ξ_1, which is a weighted average of the positions of the agents. Thus we call ξ_1 the *weighted centroid*. It is topology dependent, since the weights for the computation of ξ_1 arise from the first row of the inverse of matrix **T**. Furthermore, it is evident that $s = 0$ is a stationary root of (17) independent of the delays τ_1 and τ_2, which implies that the weighted centroid dynamics is at best marginally stable. The other factors of characteristic equation (9) are related to the *disagreement dynamics*. When these are stable the agents reach a consensus among themselves.

If the communication topology does not have a spanning tree, 1 becomes multiple eigenvalue of **C** and Eq. (17) appears as a factor multiple times within (9). These factors represent the dynamics of the centroids of the subgroups created by the subgraphs that are spanned by a tree. If all the disagreement factors are stable, the swarm members within a subgroup reach stationary positions which are generally different. Thus a consensus is not achieved. These facts are stated in the following lemmas.

Lemma 2 (*Consensusability in Case A*)**.** *Assume that the communication topology has at least one spanning tree. Then, the agents in the group reach a consensus under protocol A if and only if the factor (17) is marginally stable and all the remaining factors of (9) are stable. Furthermore, the agents reach a final group consensus value given by* $\bar{x} = \left(1/\sqrt{n}\right)\xi_1(t = \infty) = \left(1/\sqrt{n}\right)\bar{\xi}$*, whereas the other states* $\xi_j(t = \infty) = 0$ *for* $j = 2, 3, \ldots, n$.

Proof. First, we prove the necessity condition. From the definition of the new state, $\boldsymbol{\xi} = [\xi_1(t)\,\xi_2(t)\cdots\xi_n(t)]^T = \mathbf{T}^{-1}\begin{bmatrix}x_1(t)\,x_2(t)\cdots x_n(t)\end{bmatrix}^T$. If a consensus is reached, the agents have a common steady-state value. This implies that $\lim_{t\to\infty} x_j(t) = \bar{x}$, $j = 1, 2, \ldots, n$. Then

$$\lim_{t\to\infty}\begin{bmatrix}\xi_1(t) & \xi_2(t) & \cdots & \xi_n(t)\end{bmatrix}^T = \bar{x}\mathbf{T}^{-1}\begin{bmatrix}1 & 1 & \cdots & 1\end{bmatrix}^T. \quad (18)$$

Since the communication topology is assumed to have a spanning tree, 1 is a simple eigenvalue of **C**, corresponding to the eigenvector $\mathbf{t}_1 = 1\sqrt{n}\begin{bmatrix}1 & 1 & \cdots & 1\end{bmatrix}^T$, the first column of the earlier defined transformation matrix **T**. Since $\mathbf{T}^{-1}\begin{bmatrix}1 & 1 & \cdots & 1\end{bmatrix}^T = \sqrt{n}\mathbf{T}^{-1}\mathbf{t}_1 = \sqrt{n}\begin{bmatrix}1 & 0 & \cdots & 0\end{bmatrix}^T$, Eq. (18) leads to $\lim_{t\to\infty}\xi_1(t) = \sqrt{n}\bar{x}$, which indicates marginal stability for (17) and $\lim_{t\to\infty}\xi_j(t) = 0$, for $j = 2, 3, \ldots, n$, indicating asymptotic stability in the other factors of (9).

Next, the sufficiency condition is proven. If (17) is marginally stable and all the other factors in (9) are stable, the steady-state value of $\xi_1(t)$ will be constant, whereas the remaining $\xi_j(t), j = 2, 3, \ldots, n$ will tend to zero as t goes to infinity. Then, $\lim_{t\to\infty}[\xi_1(t)\,\xi_2(t)\cdots\xi_n(t)]^T = \begin{bmatrix}\bar{\xi}1 & 0 & \cdots & 0\end{bmatrix}^T$. Going back to the x domain using the inverse transformation, $\lim_{t\to\infty}\begin{bmatrix}x_1(t)\,x_2(t)\cdots x_n(t)\end{bmatrix}^T = \mathbf{T}\begin{bmatrix}\bar{\xi}1 & 0 & \cdots & 0\end{bmatrix}^T = \bar{\xi}_1\mathbf{t}_1 = \sqrt{n}\bar{x}\mathbf{t}_1 = [\bar{x}\bar{x}\cdots\bar{x}]^T$. This implies consensus. □

Lemma 3 (*Topologies Without Spanning Trees*)**.** *If the given communication topology does not have a spanning tree, the control logic described by (1) cannot result in a consensus.*

Proof. Assume that the communication topology does not have a spanning tree but instead it can be separated into $r < n$ components, i.e., disjoint subgraphs that are spanned by a tree. Then matrix **C** has 1 as a repeated eigenvalue with multiplicity r. Since **C** is stochastic, the eigenvalue 1 is always semi-simple [24], so there are r linearly independent eigenvectors corresponding to this eigenvalue. These eigenvectors are assigned to the first r columns of **T** matrix and they should have the form $\mathbf{t}_j = \begin{bmatrix}a_{j1}a_{j2}\cdots a_{jn}\end{bmatrix}^T$, $j = 1, 2, \ldots, r$, where a_{jk} is 1 if agent k belongs to the component j and 0 otherwise [25]. Each one of these r eigenvalues creates a factor of the form (17) in the characteristic equation of the system. These factors represent the dynamics of the transformed states $\xi_j(t), j = 1, 2, 3, \ldots, r$, which are at best marginally stable; recall the stationary zero characteristic root of (17).

If the remaining $n - r$ factors are all stable, the steady-state value of the system in the transformed domain is $\lim_{t\to\infty}[\xi_1(t)\,\xi_2(t)\cdots\xi_r(t)\xi_{r+1}(t)\cdots\xi_n(t)]^T = [\bar{y}_1\bar{y}_2\cdots\bar{y}_r 0\cdots 0]^T$, where $\bar{y}_j \neq \bar{y}_k$ in general. Recovering the original states using the inverse transformation, $\lim_{t\to\infty}[x_1(t)\,x_2(t)\cdots x_n(t)]^T = \mathbf{T}\begin{bmatrix}\bar{y}_1\bar{y}_2\cdots\bar{y}_m & 0\cdots 0\end{bmatrix}^T = \bar{y}_1\mathbf{t}_1 + \bar{y}_2\mathbf{t}_2 + \cdots + \bar{y}_r\mathbf{t}_r$. Due to the orthogonal construction of the $\mathbf{t}_j$ vectors and the $\bar{y}_j \neq \bar{y}_k$ condition, the agents do not reach a common state. For the degenerate case of $\bar{y}_j = \bar{y}_k$, the jth and kth subgroups have a joint steady-state behavior, but the rest of the group does not. Therefore a consensus is not achieved. □

According to Lemma 2, the characteristic polynomial given by q_1 in (17) is related to the motion of the topology-dependent centroid. The remaining factors in (9) are related to the stability of the relative motion of the agents with respect to the expected consensus. A stable swarm consensus is reached if $q_1(s, \gamma_c, \tau_1, \tau_2, \lambda_1 = 1)$ is marginally stable and all the $q_j\left(s, \gamma_c, \tau_1, \tau_2, \lambda_j\right)$, for $j = 2, \ldots, n$, are stable.

4.2. Leader tracking ability

The factorization procedure presented in the previous section also allows us to demonstrate the tracking capabilities of the control logic in cases *B*, *C*, and *D*.

As opposed to matrix **C** used in (2), matrix $\hat{\mathbf{C}}$ in (4), (6) and (8) is no longer a row-stochastic matrix, since the row sums corresponding to those agents who have access to the leader are no longer 1. This means that 1 is no longer an eigenvalue of

these matrices, and factors of the form (17) do not appear in the characteristic equation of the system. Then, all the factors created in this case can be considered as disagreement factors; if they are stable, the agents reach a common final position.

In order to show that the common position is dictated by the virtual leader, we use the fact that matrix $\hat{\mathbf{C}}$ can be augmented with column vector $\hat{\mathbf{c}}_{n+1}$ to create a new row-stochastic matrix. The proof of the following lemma details the crucial idea.

Lemma 4 (*Tracking in Protocols B, C, and D*)**.** *Assume that the communication topology has a spanning tree and that the dynamics of the disagreement factors are all stable. Then, the final positions of the agents will converge to the position of the virtual leader.*

Proof. This proof is similar to that of Lemma 2, but requires some extra definitions first. Consider the following augmented square matrix, created by the concatenation of $\hat{\mathbf{C}}$, $\hat{\mathbf{c}}_{n+1}$, and a vacuous row vector:

$$\mathbf{G} = \begin{bmatrix} \hat{\mathbf{C}} & \hat{\mathbf{c}}_{n+1} \\ \mathbf{0}_{1\times n} & 1 \end{bmatrix} \in \Re^{n+1\times n+1}, \tag{19}$$

where $\mathbf{0}_{1\times n}$ is a row vector with all its elements being zero. By construction, $\mathbf{G}$ is a row-stochastic matrix. If the communication topology has a spanning tree, of which the root has to be at the $n+1$th node, since the leader does not receive information from any agent, it is guaranteed that 1 is an eigenvalue of $\mathbf{G}$ with corresponding normalized eigenvector $\mathbf{v} = \left(1/\sqrt{n+1}\right)\mathbf{1}_{n+1}$.

Let $\mathbf{S}$ be the matrix that transforms $\mathbf{G}$ into its Jordan canonical form $\mathbf{H}$, $\mathbf{S}^{-1}\mathbf{G}\mathbf{S} = \mathbf{H}$. By construction, the eigenvalues of $\mathbf{G}$ are the same as those of $\hat{\mathbf{C}}$, with the extra 1 added by the row-stochastic property. Then we have

$$\mathbf{H} = \begin{bmatrix} \boldsymbol{\Lambda} & \mathbf{0}_{n\times 1} \\ \mathbf{0}_{1\times n} & 1 \end{bmatrix}. \tag{20}$$

And the transformation matrix is

$$\mathbf{S} = \begin{bmatrix} \mathbf{T} & \dfrac{1}{\sqrt{n+1}}\mathbf{1}_{n\times 1} \\ \mathbf{0}_{1\times n} & \dfrac{1}{\sqrt{n+1}} \end{bmatrix}, \tag{21}$$

where T is the matrix that creates the Jordan canonical form of $\hat{\mathbf{C}}$, as described in Lemma 1. Using (20) and (21), the following expression can be obtained:

$$\begin{aligned} \mathbf{S}^{-1}\mathbf{G}\mathbf{S} &= \begin{bmatrix} \mathbf{T}^{-1} & \dfrac{\mathbf{t}_{n+1}^{-1}}{\sqrt{n+1}} \\ \mathbf{0}_{1\times n} & \dfrac{1}{\sqrt{n+1}} \end{bmatrix} \begin{bmatrix} \hat{\mathbf{C}} & \hat{\mathbf{c}}_{n+1} \\ \mathbf{0}_{1\times n} & 1 \end{bmatrix} \\ &\quad \begin{bmatrix} \mathbf{T} & \dfrac{1}{\sqrt{n+1}}\mathbf{1}_{n\times 1} \\ \mathbf{0}_{1\times n} & \dfrac{1}{\sqrt{n+1}} \end{bmatrix} \\ &= \begin{bmatrix} \boldsymbol{\Lambda} & \mathbf{0}_{n\times 1} \\ \mathbf{0}_{1\times n} & 1 \end{bmatrix}, \end{aligned} \tag{22}$$

with $\mathbf{t}_{n+1}^{-1} \in \Re^n$ representing the first n rows of the last column of the inverse of matrix $\mathbf{S}$. We then define a new state transformation, including the positions of the agents and the leader:

$$\begin{aligned} \begin{bmatrix} \hat{\boldsymbol{\xi}}(t) \\ \hat{\xi}_{n+1}(t) \end{bmatrix} &= \mathbf{S}^{-1} \begin{bmatrix} \mathbf{x}(t) \\ x_{n+1}(t) \end{bmatrix} \\ &= \begin{bmatrix} \mathbf{T}^{-1} & \dfrac{\mathbf{t}_{n+1}^{-1}}{\sqrt{n+1}} \\ \mathbf{0}_{1\times n} & \dfrac{1}{\sqrt{n+1}} \end{bmatrix} \begin{bmatrix} \mathbf{x}(t) \\ x_{n+1}(t) \end{bmatrix}. \end{aligned} \tag{23}$$

From (23), we can see that the new states $\hat{\xi}_j(t)$, for $j = 1\cdots n$, will be a combination of the states of the agents with a contribution form the leader, whereas the state $\hat{\xi}_{n+1}(t)$ is only affected by the state of the leader:

$$\begin{bmatrix} \hat{\boldsymbol{\xi}}(t) \\ \hat{\xi}_{n+1}(t) \end{bmatrix} = \begin{bmatrix} \mathbf{T}^{-1}\mathbf{x}(t) + x_{n+1}(t)\,\mathbf{t}_{n+1}^{-1} \\ \sqrt{n+1}x_{n+1}(t) \end{bmatrix}. \tag{24}$$

The dynamics of the first n states is dictated by the disagreement factors generated by the eigenvalues of $\hat{\mathbf{C}}$. If they are stable, as assumed, they vanish, i.e., $\lim_{t\to\infty}\hat{\xi}_j(t) = 0$ for $j = 1\cdots n$. Then, once the transient behavior has settled, the transformed states have the form

$$\begin{bmatrix} \hat{\boldsymbol{\xi}}(\infty) \\ \hat{\xi}_{n+1}(\infty) \end{bmatrix} = \begin{bmatrix} \mathbf{0}_{n\times 1} \\ \sqrt{n+1}\,x_{n+1}(t) \end{bmatrix}. \tag{25}$$

When (25) is back transformed to obtain the actual states of the swarm members, one obtains

$$\begin{aligned} \begin{bmatrix} \mathbf{x}(t) \\ x_{n+1}(t) \end{bmatrix} &= \mathbf{S} \begin{bmatrix} \hat{\boldsymbol{\xi}}(t) \\ \hat{\xi}_{n+1}(t) \end{bmatrix} \\ &= \begin{bmatrix} \mathbf{T} & \dfrac{1}{\sqrt{n+1}}\mathbf{1}_{n\times 1} \\ \mathbf{0}_{1\times n} & \dfrac{1}{\sqrt{n+1}} \end{bmatrix} \begin{bmatrix} \mathbf{0}_{n\times 1} \\ \sqrt{n+1}x_{n+1}(t) \end{bmatrix} \\ &= \begin{bmatrix} \mathbf{1}_{n\times 1}x_{n+1}(t) \\ x_{n+1}(t) \end{bmatrix}, \end{aligned} \tag{26}$$

indicating that the n agents are tracking the leader. □

The previous result shows that, if the virtual leader settles, the agents will be able to track it in consensus when protocol *B*, *C*, or *D* is in use. However, when the leader is constantly moving, there may be some bounded tracking errors depending on the shape of the leader trajectory. The analysis of the steady-state tracking errors and their transient behaviors for different types of leader maneuver is left for future publications.

Lemmas 2–4 have shown that the proposed control laws satisfy their intended purposes provided that the factors are stable. In the following section, we deploy the Cluster Treatment of Characteristic Roots (CTCR) paradigm to solve this stability problem with respect to the time delays in an exact (i.e., non-conservative), exhaustive and efficient manner.

5. Stability analysis using the CTCR paradigm and spectral delay space domain

This section is devoted to the stability analysis of the individual factors generated in each case. First, we present a brief review of the CTCR paradigm and the novel concept of spectral delay space (SDS). Then, we show how this technique is applied to the specific problem at hand, making a special distinction in the case of (16a) and (16b).

5.1. Brief review of the CTCR paradigm

The main philosophy behind the Cluster Treatment of Characteristic Roots (CTCR) paradigm [14,15] is the "clustering" of all possible imaginary root crossings in the $(\tau_1, \tau_2) \in \Re^{2+}$ domain for a given linear time-invariant multiple time delay system. It pertains to any quasi-polynomial characteristic equation, such as (15a) or (15b). The method starts with the exhaustive determination of such crossings, and then takes advantage of their special features. The following paragraphs present some preparatory definitions and the key propositions of the CTCR paradigm.

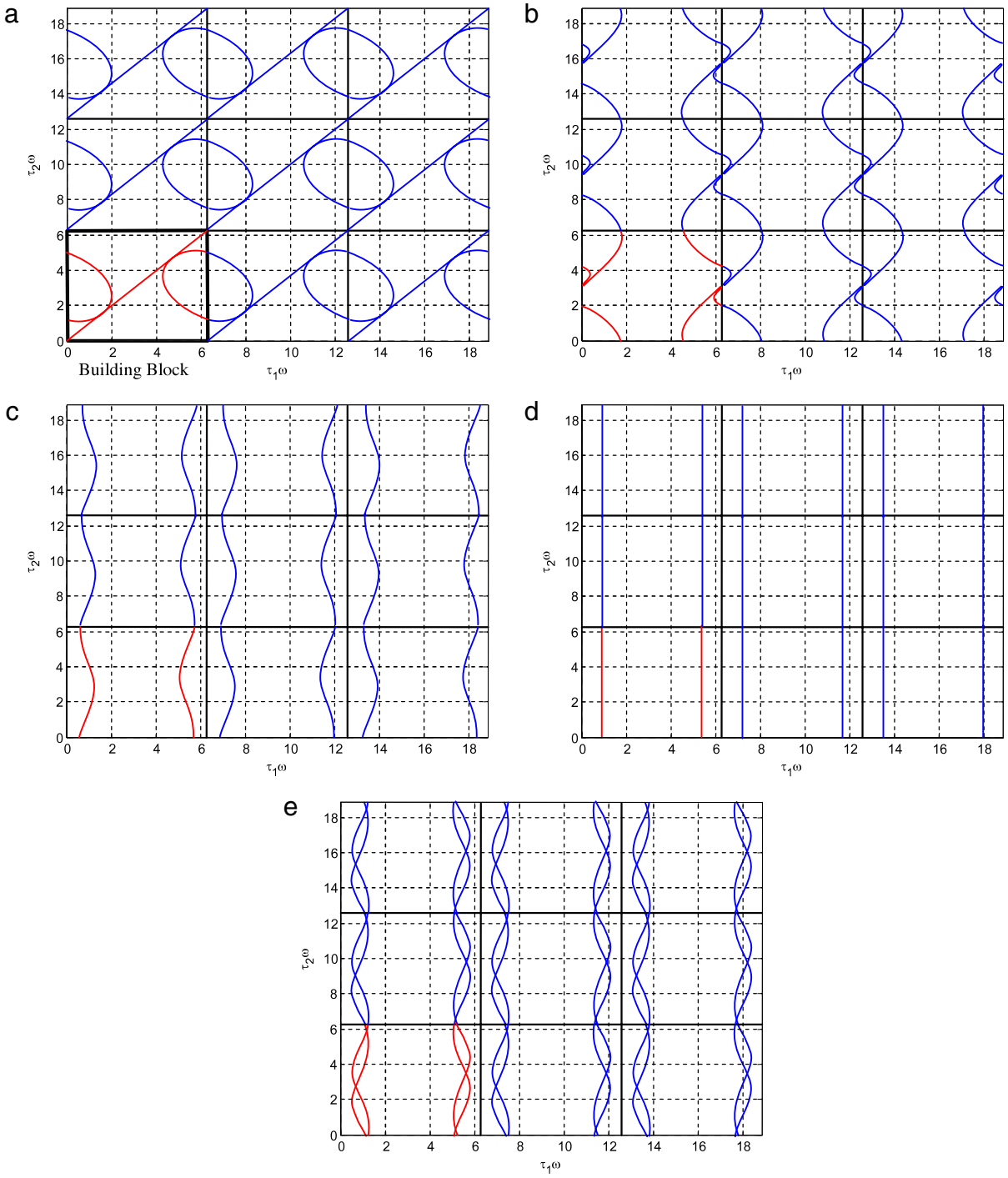

Fig. 1. SDS representation of the stability switching curves of six agents interacting under protocol *A*. (a) $\lambda = 1$, (b) $\lambda = -0.846$, (c) $\lambda = 0.295$, (d) $\lambda = -0.003$, and (e) $\lambda = -0.233 \pm 0.255i$. Red: building hypercurves; blue: reflection hypercurves. (For interpretation of the references to colour in this figure legend, the reader is referred to the web version of this article.)

Definition 1 (*Kernel Hypercurves* $\wp_0$)**.** The curves that consist of *all* the points $(\tau_1, \tau_2) \in \Re^{2+}$, exhaustively, which cause an imaginary root $s = \omega i, \omega \in \Re^+$ and satisfy the constraint $0 < \tau_k\omega < 2\pi$, are called the *kernel curves*. The points on this curve contain the smallest delay compositions which correspond to all possible imaginary roots.

Definition 2 (*Offspring Curves* $\wp$)**.** The curves obtained from the kernel curve by the following pointwise nonlinear transformation,

$$\left\langle \tau_1 \pm \frac{2\pi}{\omega} j_1,\ \tau_2 \pm \frac{2\pi}{\omega} j_2 \right\rangle, \quad j_1, j_2 = 0, 1, 2, \ldots, \tag{27}$$

are called the *offspring hypercurves*.

Definition 3 (*Root Tendency, RT*)**.** The root tendency indicates the direction of transition of the imaginary root as only one of the delays, τ_j, increases by ε, $0 < \varepsilon \ll 1$, while all the others remain constant:

$$RT\,|_{s=\omega i}^{\tau_j} = \operatorname{sgn}\left[\operatorname{Re}\left(\frac{\partial s}{\partial \tau_j}\bigg|_{s=\omega i}\right)\right]. \tag{28}$$

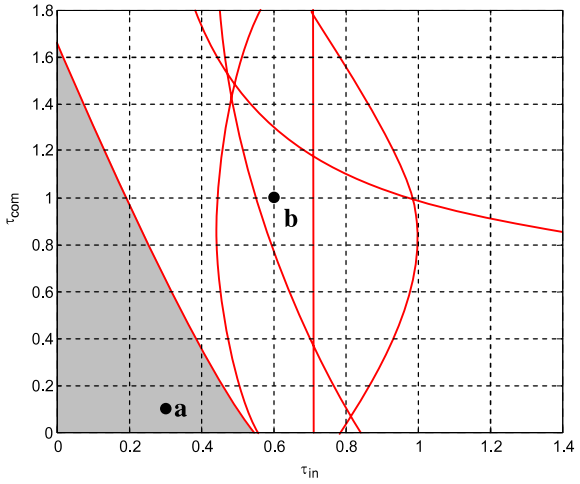

Fig. 2. Stability map for protocol *A* and in the domain of the time delays. The shaded zone represents the stable region.

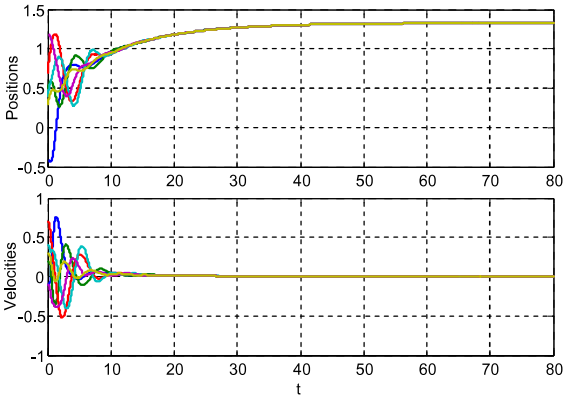

Fig. 3. Traces of the agents operating under protocol *A* with a stable delay combination corresponding to point **a** in Fig. 2.

There are two overarching propositions which support the CTCR paradigm. We will state them here from [14] without proof.

Proposition 1 (*Small Number of Kernel Hypercurves*)**.** *The number of kernel hypercurves is manageably small. To be specific, for a linear time-invariant time delay system of state dimension n, the maximum possible number of kernel hypercurves is* n^2 [26].

Proposition 2 (*Invariant Root Tendency Property*)**.** *Take an imaginary characteristic root,* ωi*, caused by any one of the infinitely many grid points on the kernel and offspring hypercurves in* $(\tau_1, \tau_2) \in \Re^{2+}$ *defined by expression* (27)*. The root tendency of these imaginary roots remains invariant from one* 'offspring hypercurve' *to the other when one of the delays is kept constant. That is, the root tendency with respect to the variations of* τ_1 *(or* τ_2*) is invariant from the kernel to the corresponding offspring as* τ_2 *(or* τ_1*) is fixed.*

5.2. Spectral delay space (SDS)

As we mentioned earlier, the first step required for the deployment of the CTCR paradigm is to find exhaustively all the potential stability switching curves, i.e., the kernel and offspring. A new procedure is described in this segment of the preparations. It is a formalized treatment from a recent thesis work [15,27]. The procedure is developed on a new domain: the *spectral delay space* (SDS). It is defined by the coordinates $v_j = \tau_j \omega$ for every

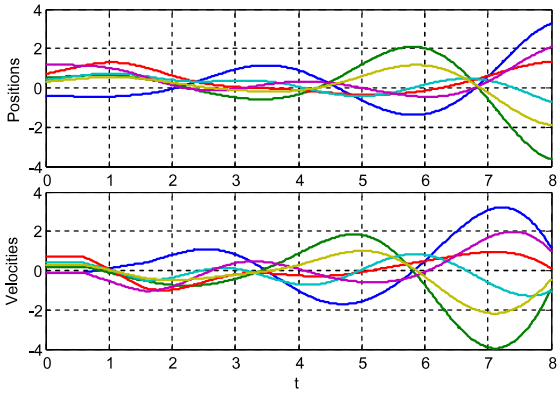

Fig. 4. Traces of the agents operating under protocol *A* with an unstable delay combination corresponding to point **b** in Fig. 2.

point $(\tau_1, \tau_2) \in \Re^{2+}$ on the kernel or the offspring curves. This transformation presents a conditional mapping: if a delay set (τ_1, τ_2) creates an imaginary root ωi, (i.e., if the point is on the kernel or the offspring curves) then $(\tau_1\omega, \tau_2\omega)$ forms a point in the SDS. In contrast, (τ_1, τ_2) points that do not generate an imaginary root have no representation in the SDS.

The main advantage of the SDS is that the representation of the kernel curve in the SDS, denoted as $\wp_0^{SDS}$ and called the *building curve*, is confined into a square of edge length 2π. Then, it is only necessary to explore a finite domain to find the representation of the building curves in the SDS. This finite domain is known as the *building block* (BB), i.e., $2\pi \times 2\pi$ squares, as per (27). Another advantage of these coordinates is that the transitions from the *building* to the *reflection* curves (i.e., the representation of the *offspring* curves in the SDS) is achieved simply by stacking the copies of the BB as opposed to using the pointwise nonlinear transformation (27), which results in an undesirable shape distortion. There are several other intriguing properties of the SDS and BB concepts which can be found in [15].

5.3. Stability analysis of the factors

We now deploy the CTCR method to the factors of the characteristic equation, using the SDS concept. For this, we follow the mathematical procedure described in the Appendix of [27] which evaluates the building curves.

As an example, let us take the factor in (15a). For a certain eigenvalue λ_i and parameter γ, it can be expressed in a generic form (suppressing λ_i and γ terms) as

$$q_j(s, \tau_1, \tau_2) = d_1(s) + d_2(s)\, e^{-\tau_1 s} + d_3(s)\, e^{-\tau_2 s} = 0, \tag{29}$$

where the $d_i(s), i = 2, 3$, terms represent the expressions multiplying the respective exponential terms, and $d_1(s)$ is the polynomial of s free of transcendental terms.

In order to obtain the imaginary roots of (29), $s = \omega i$ is substituted. Then, the exponential terms are replaced by

$$e^{-\tau_k \omega i} = \cos(v_k) - i \sin(v_k), \quad v_k = \tau_k \omega, k = 1, 2, \tag{30}$$

and the sine and cosine functions are expressed in parameterized form of the half-angle tangent function:

$$\cos(v_k) = \frac{1 - z_k^2}{1 + z_k^2}, \qquad \sin(v_k) = \frac{2z_k}{1 + z_k^2},$$
$$z_k = \tan(v_k/2). \tag{31}$$

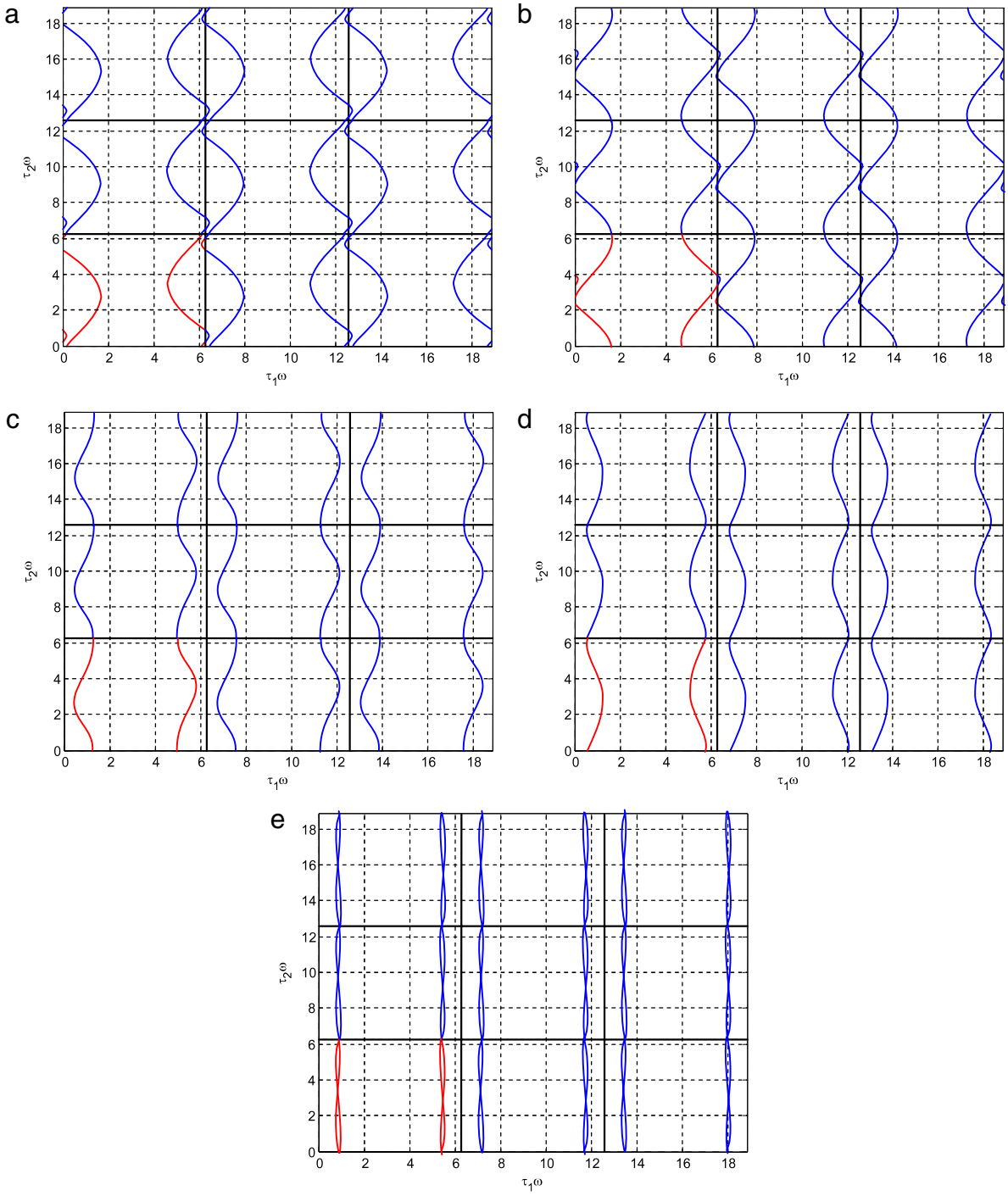

Fig. 5. SDS representation of the stability switching curves of six agents interacting under protocol B or C. (a) $\lambda = 0.731$, (b) $\lambda = -0.697$, (c) $\lambda = -0.388$, (d) $\lambda = 0.332$, and (e) $\lambda = 0.011 \pm 0.032i$. Red: building hypercurves; blue: reflection hypercurves. (For interpretation of the references to colour in this figure legend, the reader is referred to the web version of this article.)

Eq. (29) can now be written as a polynomial in ω:

$$q_j(\omega, z_1, z_2) = \sum_{k=0}^{2} c_k(\gamma, \lambda_j, z_1, z_2)(\omega i)^k = 0, \tag{32}$$

where c_k is the coefficient of the kth power of ωi, parameterized in γ, λ_j, z_1,and z_2. Notice that (15a) is quadratic in free s terms; thus the power of ωi goes up to 2 in (32). If there is a solution $\omega \in \Re^+$ to (32), it will represent an imaginary root of (29). For such a root, both the real and imaginary parts of (32) must be zero simultaneously:

$$\mathrm{Re}\left[q_j(\omega, z_1, z_2)\right] = \sum_{k=0}^{2} f_k(z_1, z_2)\omega^k = 0 \tag{33a}$$

$$\mathrm{Im}\left[q_j(\omega, z_1, z_2)\right] = \sum_{k=0}^{2} g_k(z_1, z_2)\omega^k = 0, \tag{33b}$$

where $f_k(z1, z2)$ and $g_k(z1, z2)$ symbolize the coefficients of the powers of ω in the respective equations. The condition for (33a)

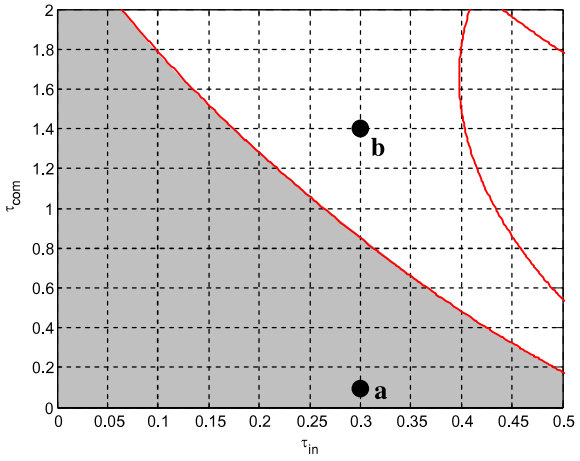

Fig. 6. Stability map for protocols B and C in the domain of the time delays. The shaded zone represents the stable region.

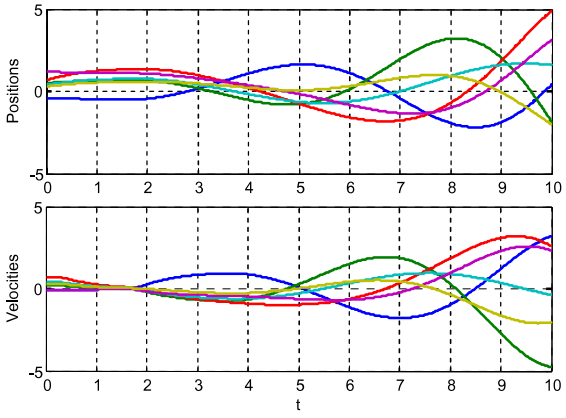

Fig. 8. Traces of the agents in the consensus regulation case with an unstable delay combination corresponding to point **b** in Fig. 6.

and (33b) to share a common root is simply stated using a Sylvester's resultant matrix:

$$\mathbf{M} = \begin{bmatrix} f_2(z_1,z_2) & f_1(z_1,z_2) & f_0(z_1,z_2) & 0 \\ 0 & f_2(z_1,z_2) & f_1(z_1,z_2) & f_0(z_1,z_2) \\ g_2(z_1,z_2) & g_1(z_1,z_2) & g_0(z_1,z_2) & 0 \\ 0 & g_2(z_1,z_2) & g_1(z_1,z_2) & g_0(z_1,z_2) \end{bmatrix}. \tag{34}$$

In order for (33a) and (33b) to be satisfied, **M** should be singular. This results in the following expression in terms of z_1 and z_2:

$$F(z_1,z_2) \stackrel{def}{=} \det(\mathbf{M}) = F(\tan(v_1/2), \tan(v_2/2)) = 0, \tag{34a}$$

which constitutes a closed-form description of the kernel curves in the SDS (v_1, v_2), i.e., the building curves. To obtain its graphical depiction, one of the parameters, say v_2, can be scanned in the range of $[0, 2\pi]$, and the corresponding v_1 values are calculated again in $[0, 2\pi]$. Notice that every point (v_1, v_2) on these curves brings an imaginary characteristic root at $\pm\omega i$ which can be evaluated from (33a) or (33b). Through this process we create a continuous sequence of (v_1, v_2, ω) along the kernel curves. We then back transform from the SDS domain (v_1, v_2) to the delay space (τ_1, τ_2), using the inverse transformation of (30) with the appropriate ω values. This generates the kernel and offspring curves.

The kernel and offspring curves divide the (τ_1, τ_2) domains into regions of possible stability and instability. To determine the stability nature of these regions, we start from the non-delayed system (i.e., $\tau_1 = \tau_2 = 0$). The quadratic expression (15a) is always stable because $\lambda_j \leq 1$ and $\gamma > 0$ (except the case when $\lambda_j = 1$, which creates double roots at the origin). If one also considers the non-delayed behavior of the factor given in Eq. (15b), it reads as

$$q_j(s,\gamma,\tau_1,\tau_2,\lambda_j) = s^4 + 2s^2(\gamma s+1)(1-\mathrm{Re}(\lambda_j)) + (\gamma s+1)^2\left(1-2\mathrm{Re}(\lambda_j)+|\lambda_j|^2\right) = 0. \tag{35}$$

Conventional deployment of Routh's array results in the following necessary and sufficient condition for this non-delayed behavior to be stable:

$$\gamma > \bar{\gamma} = \max_{\substack{\lambda_j \neq 1 \\ j=1\cdots n}} \sqrt{\frac{\mathrm{Im}(\lambda_j)^2}{(1-\mathrm{Re}(\lambda_j))((\mathrm{Re}(\lambda_j)-1)^2+\mathrm{Im}(\lambda_j)^2)}}. \tag{36}$$

This bound is clearly known to facilitate the selection of a proper γ, as we will demonstrate in the examples later.

Since the homogeneous dynamics of protocols A, B, and C are identical, (36) applies to all three of them. A similar condition can be easily obtained for protocol D using Eq. (16b).

Starting from the non-delayed case, one can follow a practical path (for instance parallel to τ_1 axis, and varying only τ_2), and determine the root tendencies on the kernel hypersurfaces

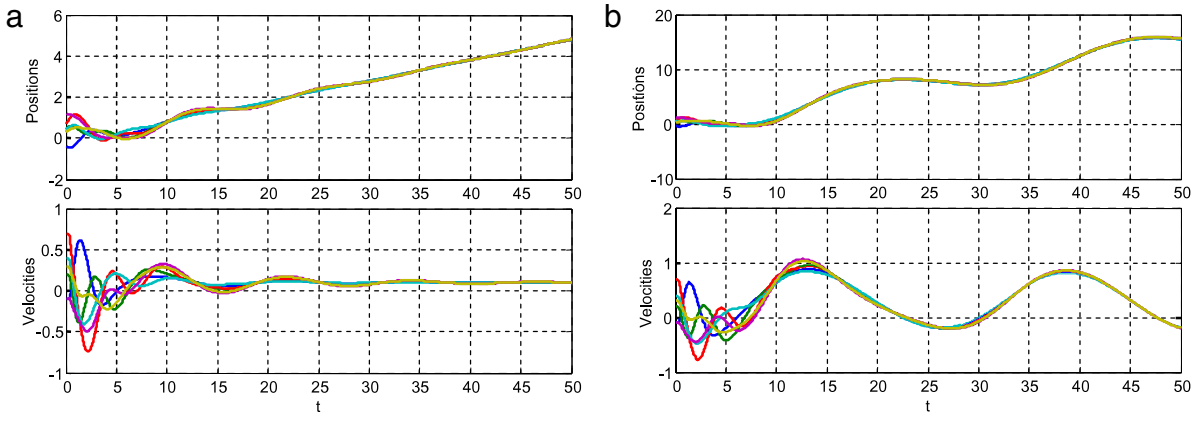

Fig. 7. Traces of the agents operating under protocols B and C with a stable delay combination corresponding to point **a** in Fig. 6. (a) Consensus regulation (protocol B) case. (b) Tracking with full access (protocol C) case.

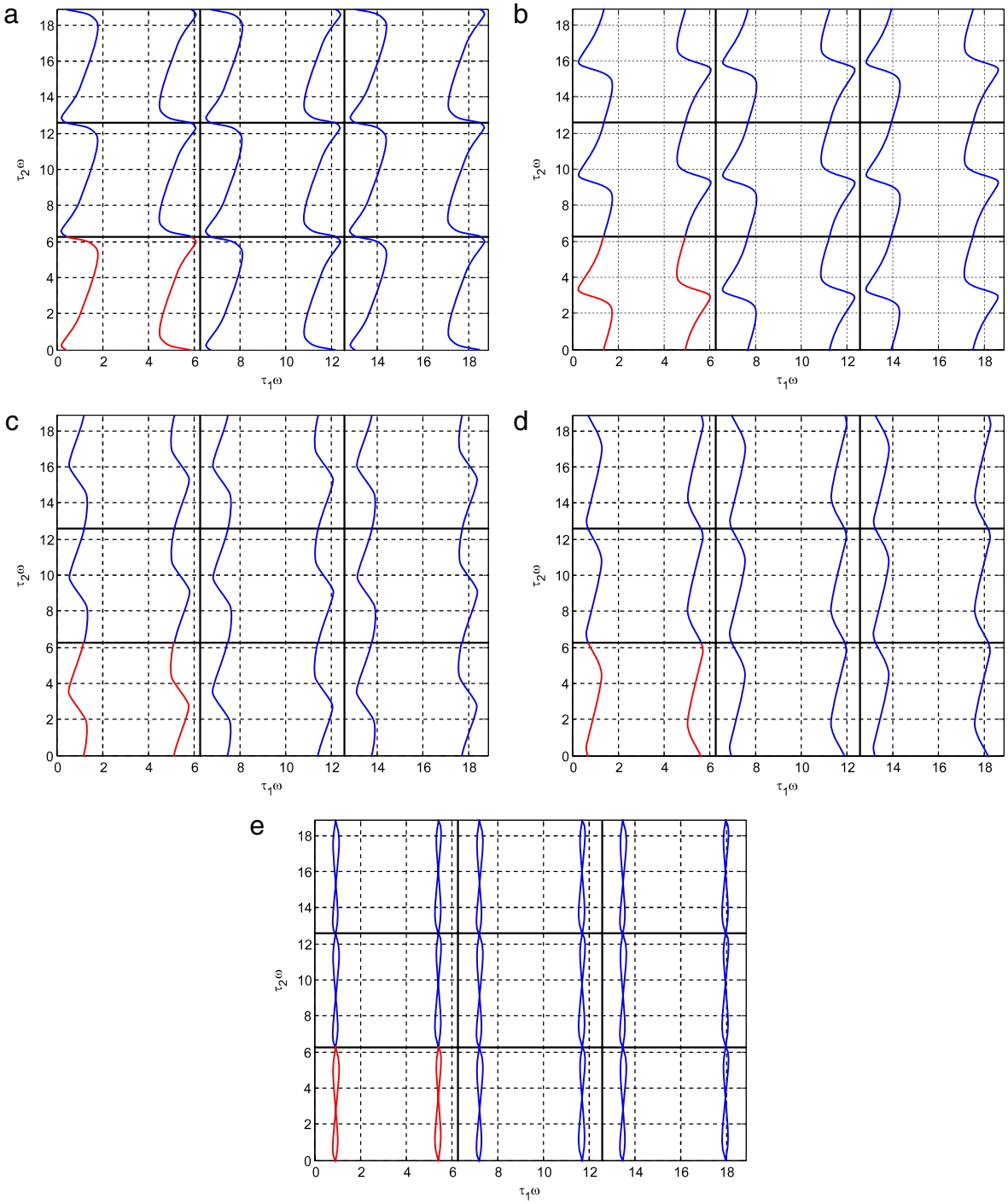

Fig. 9. SDS representation of the stability switching curves of six agents interacting under protocol *D*. (a) $\lambda = 0.731$, (b) $\lambda = -0.697$, (c) $\lambda = -0.388$, (d) $\lambda = 0.332$, and (e) $\lambda = 0.011 \pm 0.032i$. Red: building hypercurves; blue: reflection hypercurves. (For interpretation of the references to colour in this figure legend, the reader is referred to the web version of this article.)

(which are in small number as per Proposition 1). The root tendency invariance property (Proposition 2 in Section 5.1) is then deployed from one region to the other. This yields a complete and exact stability outlook of the factors in the space of the delays, $(\tau_1, \tau_2) \in \Re^{2+}$.

5.4. The special case D: neutral factors

The application of the CTCR to the factors generated by protocols *A*, *B*, and *C* has no particularities. They are *retarded-type multiple time delay systems*, and their stability analysis is performed as explained above. The factors created by protocol *D*, however, belong to a special case, and they need to be treated differently.

As mentioned earlier, in (8), (16a) and (16b) the highest derivative of the state, and the highest degree of *s*, are accompanied by delay terms. This fact makes this system a *neutral-type multiple time delay System* (NMTDS), the generic form of which can be presented as

$$\dot{\mathbf{x}}(t) = \mathbf{A}\mathbf{x}(t) + \mathbf{B}_1\mathbf{x}(t-\tau_1) + \mathbf{B}_2\mathbf{x}(t-\tau_2) + \mathbf{D}\dot{\mathbf{x}}(t-\tau_2). \quad (37)$$

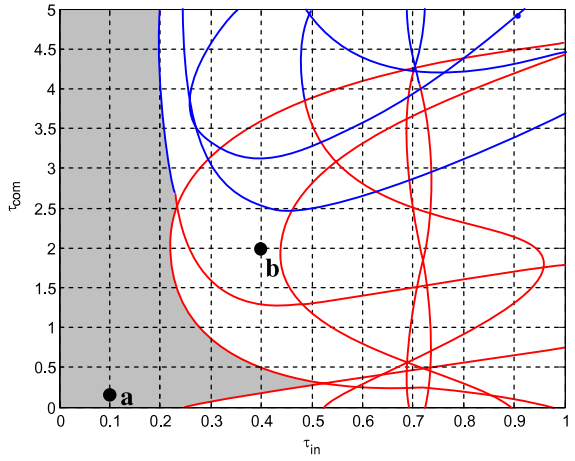

Fig. 10. Stability map for protocol *D* in the domain of the time delays. The shaded zone represents the stable region.

The feature of an NMTDS that discriminates it from the retarded class is that an NMTDS which is asymptotically stable for the non-delayed case may not be stable for infinitesimally small delays while the retarded class is always stable. If that is the case, the system will have infinitely many unstable characteristic roots for any value of the delays, and further stability analysis is not required.

A necessary condition for an NMTDS system like (37) to be stable for small delays (also known as the *delay stabilizability* feature), is that the discrete operator

$$\mathbf{x}(t) - \mathbf{D}\mathbf{x}(t - \tau_2) = 0 \tag{38}$$

must be stable. This condition can be obtained as a consequence of the application of the CTCR propositions, as proven in [19]. In essence, the stability of (38) is guaranteed if the spectral radius of matrix **D** is less than 1. In the case of the subsystems created after the factorization procedure is applied to case *D*, we observe that the **D** matrix is either

$$\lambda_j \begin{bmatrix} 0 & 0 \\ 0 & 1 \end{bmatrix} \tag{39}$$

for real eigenvalues of matrix $\hat{\mathbf{C}}$, or

$$\begin{bmatrix} \mathrm{Re}(\lambda_j) & -\mathrm{Im}(\lambda_j) \\ -\mathrm{Im}(\lambda_j) & \mathrm{Re}(\lambda_j) \end{bmatrix} \otimes \begin{bmatrix} 0 & 0 \\ 0 & 1 \end{bmatrix} \tag{40}$$

in the case of complex conjugate eigenvalues. By using Gershgorin's disk theorem, it is easy to see that the norms of the eigenvalues of $\hat{\mathbf{C}}$ are always strictly less than 1, and therefore the spectral radius of matrices (39) and (40) is less than 1. This implies that the factors created by protocol *D* are delay stabilizable.

Once this stabilizability condition is satisfied, the deployment of the CTCR for this case follows exactly the same steps as in the retarded systems, described in the previous segment. The end result, again, is a unique non-conservative and exhaustive stability table for these group dynamics in the domain of the independent delays. The following section presents some numerical examples which validate the results.

6. Example cases

The results of some numerical simulations are presented here to validate the analytical developments. We borrow the examples from [8]. A group of six agents is considered. The following adjacency matrix is used for the leaderless consensus problem (case *A*):

$$\mathbf{A}_\Gamma = \begin{bmatrix} 0 & 5 & 0 & 2.5 & 0 & 2.5 \\ 8 & 0 & 1 & 0 & 1 & 0 \\ 0 & 2 & 0 & 2 & 3 & 3 \\ 1 & 0 & 1 & 0 & 8 & 0 \\ 0 & 1.2 & 0 & 1.8 & 0 & 7 \\ 5 & 1 & 0 & 2 & 2 & 0 \end{bmatrix}, \tag{41}$$

and for the leader–follower examples (cases *B*, *C*, and *D*) we use

$$\mathbf{A}_{\Gamma+1} = \begin{bmatrix} 0 & 1 & 0 & 1 & 0 & 0 & 1 \\ 8 & 0 & 1 & 0 & 1 & 0 & 0 \\ 0 & 3 & 0 & 0 & 0 & 3 & 4 \\ 1 & 0 & 0 & 0 & 1 & 0 & 8 \\ 0 & 1.2 & 0 & 1.8 & 0 & 7 & 0 \\ 5 & 1 & 0 & 0 & 4 & 0 & 0 \end{bmatrix}. \tag{42}$$

6.1. Leaderless consensus

Matrix **C** generated by (41) has eigenvalues 1, 0.295, −0.003, −0.846, and $-0.223 \pm 0.255i$. The control gain is selected as $\gamma = 1$, well beyond the lower bound $\bar{\gamma} = 0.192$ defined by (36). After the procedure described in Section 5 is applied, the building and reflection curves in SDS for each one of the factors are obtained. They are presented in Fig. 1.

Then, by mapping these curves to the (τ_1, τ_2) domain, and to the original (τ_{in}, τ_{com}) space, the stability tables for all the factors in (9) are created. These stability tables are later superposed to generate the complete stability map for the system, as displayed in Fig. 2.

To validate this stability analysis, we reproduce one of the example cases presented in [8]. The point **a** in Fig. 2

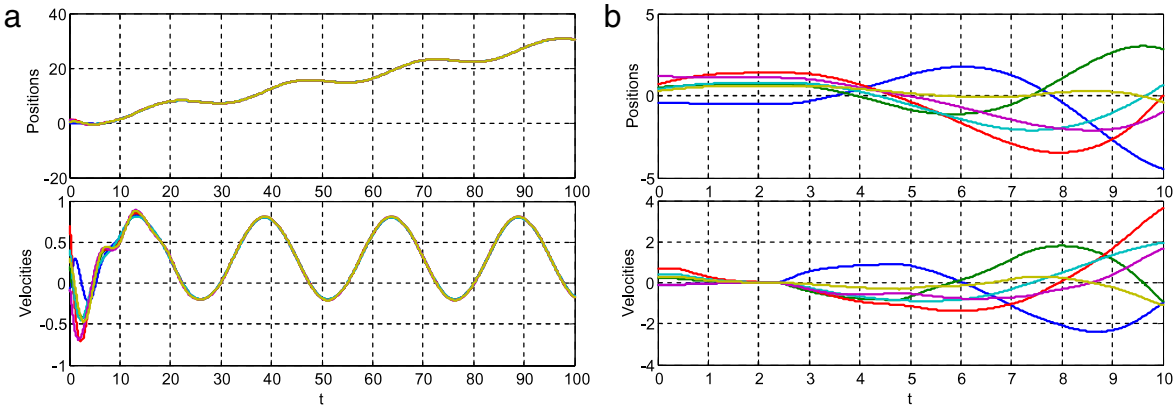

Fig. 11. Traces of the agents operating under protocol *D*. (a) Stable delay combination, point **a** in Fig. 10; (b) unstable delay combination, point **b** in Fig. 10.

($\tau_{in} = 0.3$, $\tau_{com} = 0.1$) represents a stable behavior. Fig. 3 shows the traces of the agents, which are obtained using the same initial conditions as in the referred paper. It is identical to Fig. 2(a) in [8].

Furthermore, Fig. 4 shows the traces for delay values selected at point **b** in Fig. 2. This point is outside the shaded region, and thus it is an unstable operating point, as is demonstrated by the traces in Fig. 4.

Certainly, Fig. 2 is a more comprehensive and exhaustive stability result than that presented by Theorem 5.1 of [8]. This exact and exhaustive stability map is made possible by deploying the unique features of the CTCR paradigm.

6.2. Consensus regulation and tracking with full access

The stability analysis for cases *B* and *C* is the same, since the homogeneous parts of systems (4) and (6) are identical. Matrix $\hat{\mathbf{C}}$ created from (42) has eigenvalues -0.6972, -0.3883, 0.3323, 0.7311, and $-0.011 \pm 0.0322i$. The SDS representation of the imaginary crossings for these factors is given in Fig. 5, and the corresponding stability map in the domain of the delays is in Fig. 6. Again, the stability results presented here are more precise than those in [8], and we do not require the pursuit of a different stability criterion for each protocol.

We also reproduce the tracking results from [8], using $x_d(t) = -0.2 + 0.1t$ for case *B*, consensus regulation (constant leader velocity), and $x_d(t) = -0.2 + 0.3t - 1.6\sin(t/4)$ for case *C*, consensus tracking with full access to the virtual leader; the traces of the agents in these cases are shown in Fig. 7. They are operating with a delay composition of ($\tau_{in} = 0.3$, $\tau_{com} = 0.1$), corresponding to point **a** in Fig. 6.

As an example of an unstable delay combination, Fig. 8 shows the traces of the agents operating under protocol *B*, with a delay combination of ($\tau_{in} = 0.3$, $\tau_{com} = 1.4$), point **b** in Fig. 6, which clearly represents an unstable operating point.

6.3. Consensus tracking with partial access

For case *D*, the same matrix (42) is used. Here, of course, the stability outlook is different from that of the previous subsection because of the different structure of the factors. The SDS representation for this case is shown in Fig. 9, and the corresponding stability chart in the domain of the delays is given in Fig. 10. In this figure we also visit the "*delay scheduling*" concept [16,17]. Imagine that the present delays are ($\tau_{in} = 0.4$, $\tau_{com} = 0.1$), and that this setting imposes unstable consensus according to Fig. 10. The CTCR method provides the control option of artificially prolonging the delays to ($\tau_{in} = 0.4$, $\tau_{com} = 0.4$) in order to regain the stability. Since this is a practicable operation, such delay scheduling steps can be used as an effective tool in multi-agent dynamics. We leave further details of this deployment to other investigations, due to space limitations here.

Notice again that in this paper we have considered both time delays for case *D*, as opposed to the single delay treatment of [8], where the agents were assumed to be affected only by the communication delay. This is a demonstrable advantage of using the CTCR paradigm over the Lyapunov-based techniques. However, the shaded region in Fig. 10 includes the axis $\tau_{in} = 0$, meaning that in this case the system is stable independently of τ_{com}. This verifies the result of Theorem 5.4 in [8], where the system is proven to be delay-independent stable provided that some conditions are satisfied. That is obviously the case for the example case selected and reproduced here.

Fig. 11 shows the traces of the agents tracking the virtual leader for stable (Fig. 11(a)) and unstable (Fig. 11(b)) delay compositions, belonging to points **a** and **b** in Fig. 10, respectively.

7. Conclusion

This paper investigates four different consensus protocols for multi-agent systems, from several novel perspectives. The agents communicate through a directed network. Their dynamics is affected by a communication delay and an input delay which are rationally independent. The first delay influences the information coming from the peer agents, whereas the second one appears in both its own state and the state of the informers.

Earlier performed conservative stability analysis, based on the Razumikhin theorem, is replaced here with a novel technique that decouples the dynamics into a set of second-order and fourth-order subsystems. Then the CTCR paradigm is deployed on these subsystems which are discriminated from each other only by a parameter. These parameters happen to be the eigenvalues of a certain matrix which is related to the communication topology only. Utilizing these eigenvalues, we factorize the characteristic equation of the group dynamics in some generic primitives (factors). We then use a practical paradigm, CTCR, for stability assessment of each factor.

The deployment of the CTCR takes advantage of the spectral delay space concept to generate an exact and exhaustive stability map of each factor in the domain of the time delays efficiently. Example cases validate the technique.

References

[1] R. Olfati-Saber, R. Murray, Consensus problems in networks of agents with switching topology and time delay, IEEE Transactions on Automatic Control 49 (8) (2004) 1520–1533.
[2] W. Ren, R.W. Beard, Consensus seeking in multi-agent systems under dynamically changing interaction topologies, IEEE Transactions on Automatic Control 50 (5) (2005) 655–661.
[3] Y. Sun, L. Wang, Consensus problems in networks of agents with double integrator dynamics and time varying delays, International Journal of Control 82 (9) (2009) 1937–1945.
[4] Y. Sun, L. Wang, Consensus of multi-agent systems in directed networks with non-uniform time-varying delays, IEEE Transactions on Automatic Control 54 (7) (2009) 1607–1613.
[5] R. Cepeda-Gomez, N. Olgac, An exact methodology for the stability analysis of linear consensus protocols with time delay, IEEE Transactions on Automatic Control 56 (7) (2011) 1734–1740.
[6] R. Cepeda-Gomez, N. Olgac, Exhaustive stability analysis in a consensus system with time delay and irregular topologies, International Journal of Control 84 (4) (2011) 746–757.
[7] R. Cepeda-Gomez, N. Olgac, Consensus analysis with large and multiple communication delays using spectral delay space (SDS) concept, International Journal of Control 84 (12) (2011) 1996–2007.
[8] Z. Meng, W. Ren, Y. Cao, Y. Zheng, Leaderless and leader–follower consensus with communication and input delays under a directed network topology, IEEE Transactions on Systems Man and Cybernetics—Part B 41 (1) (2011) 75–88.
[9] Y. Tian, C. Liu, Consensus of multi-agent systems with diverse input and communication delays, IEEE Transactions on Automatic Control 53 (2008) 2122–2128.
[10] Y. Tian, C. Liu, Robust consensus of multi-agent systems with diverse input delays and asymmetric interconnection perturbations, Automatica 43 (2009) 1347–1353.
[11] J.K. Hale, S.M. Verduyn-Lunel, Introduction to Functional Differential Equations, Springer Verlag, New York, 1993.
[12] U. Münz, A. Papachristodoulou, F. Allgower, Delay robustness in consensus problems, Automatica 45 (2010) 1252–1265.
[13] N. Olgac, R. Sipahi, The cluster treatment of characteristic roots and the neutral type time-delayed systems, Journal of Dynamics, Measurement and Control—Transactions of the ASME 127 (2005) 88–97.
[14] R. Sipahi, N. Olgac, A unique methodology for the stability robustness of multiple time delay systems, Systems and Control Letters 55 (10) (2006) 819–825.
[15] H. Fazelinia, R. Sipahi, N. Olgac, Stability robustness analysis of multiple time-delayed systems using building block concept, IEEE Transactions on Automatic Control 52 (5) (2007) 799–810.
[16] N. Olgac, R. Sipahi, A.F. Ergenc, Delay scheduling, an unconventional use of time delay for trajectory tracking, Mechatronics 17 (4–5) (2007) 199–206.
[17] N. Olgac, A.F. Ergenc, R. Sipahi, Delay scheduling: a new concept for stabilization in multiple time delay systems, Journal of Vibration and Control 11 (9) (2005) 1159–1172.

[18] R.D. Schaefer, An Introduction to Nonassociative Algebras, Dover, New York, 1996.
[19] N. Olgac, T. Vyhlidal, R. Sipahi, A new perspective in the stability assessment of neutral systems with multiple and cross-talking delays, SIAM Journal of Control and Optimization 47 (1) (2008) 327–344.
[20] W. Michiels, T. Vyhlídal, An eigenvalue based approach for the stabilization of linear time-delay systems of neutral type, Automatica 41 (2005) 991–998.
[21] O. Toker, H. Ozbay, Complexity issues in robust stability of linear delay-differential systems, Mathematics of Control, Signals and Systems 9 (4) (1996) 386–400.
[22] M. Marcus, H. Minc, A Survey of Matrix Theory and Matrix Inequalities, Dover, New York, 1996.
[23] H.E. Bell, Gershgorin's theorem and zeros of polynomials, American Mathematical Monthly 74 (1965) 292–295.
[24] R. Agaev, P.W. Chebotarev, On the spectra of nonsymmetric Laplacian matrices, Linear Algebra and its Applications 399 (2005) 157–168.
[25] N. Biggs, Algebraic Graph Theory, Cambridge University Press, New York, 1993.
[26] A.F. Ergenc, N. Olgac, H. Fazelinia, Extended Kronecker summation for cluster treatment of LTI systems with multiple delays, SIAM Journal on Control and Optimization 46 (1) (2007) 143–155.
[27] H. Fazelinia, A novel stability analysis of systems with multiple time delays and its application to high speed milling chatter, Ph.D. Dissertation, University of Connecticut, Storrs, Connecticut, 2007.